The Focusing Optics x-ray Solar Imager: FOXSI

Säm Krucker[a,b], Steven Christe[c], Lindsay Glesener[a,d], Shin-nosuke Ishikawa[a], Stephen McBride[a], David Glaser[a], Paul Turin[a], R. P. Lin[a,d,e], Mikhail Gubarev[f], Brian Ramsey[f] Shinya Saito[g,h], Yasuyuki Tanaka[g], Tadayuki Takahashi[g,h], Shin Watanabe[g,h], Takaaki Tajima[i] , Hiroyasu Tajima[j], Satoshi Masuda[j]

[a]Space Sciences Lab, U.C. Berkeley, 7 Gauss Way, Berkeley, CA 94720-7450, USA
[b]University of Applied Sciences Northwestern Switzerland, CH-5210 Windisch, Switzerland
[c]Solar Physics Laboratory, NASA/GSFC, Greenbelt, MD 20771-0001, USA
[d]Physics Department, U.C. Berkeley, Berkeley, CA 94720, USA
[e]School of Space Research, Kyung Hee University, Yongin, Gyeonggi, Korea
[f]Space Science Department, NASA/MSFC, Huntsville, AL 35812, USA
[g]Institute of Space and Astronautical Science, Sagamihara, Kanagawa, 252-5210, Japan
[h]Department of Physics, University of Tokyo, Hongou, Bunkyo-ku, Tokyo, 113-0033, Japan
[i]KIPAC, Stanford University, Stanford, CA 94305, USA
[j]STEL, Nagoya University, Furo-cho, Chikusa-ku, Nagoya 464-8601, Japan

ABSTRACT

The Focusing Optics x-ray Solar Imager (FOXSI) is a sounding rocket payload funded under the NASA Low Cost Access to Space program to test hard x-ray (HXR) focusing optics and position-sensitive solid state detectors for solar observations. Today's leading solar HXR instrument, the Reuven Ramaty High Energy Solar Spectroscopic Imager (RHESSI) provides excellent spatial (2 arcseconds) and spectral (1 keV) resolution. Yet, due to its use of an indirect imaging system, the derived images have a low dynamic range (typically <10) and sensitivity. These limitations make it difficult to study faint x-ray sources in the solar corona which are crucial for understanding the particle acceleration processes which occur there. Grazing-incidence x-ray focusing optics combined with position-sensitive solid state detectors can overcome both of these limitations enabling the next breakthrough in understanding impulsive energy release on the Sun. The FOXSI project is led by the Space Sciences Laboratory at the University of California, Berkeley. The NASA Marshall Space Flight Center is responsible for the grazing-incidence optics, while the Astro-H team at JAXA/ISAS has provided double-sided silicon strip detectors. FOXSI is a pathfinder for the next generation of solar hard x-ray spectroscopic imagers. Such observatories will be able to image the non-thermal electrons within the solar flare acceleration region, trace their paths through the corona, and provide essential quantitative measurements such as energy spectra, density, and energy content in accelerated electrons.

Keywords: sounding rocket payload, solar physics, solar flares, silicon strip detectors, grazing-incidence optics, high-energy x-ray optics, electroform-nickel replication

1. INTRODUCTION

Hard x-ray (HXR) observations are a powerful diagnostic tool providing quantitative measurements of non-thermal energetic (>10 keV) electrons, in particular for electrons accelerated in solar flares. Energetic electrons traveling in a plasma radiate HXR emission through the well-known process of bremsstrahlung. In solar flares, it is thought that electrons are accelerated somewhere in the solar atmosphere (the corona) and travel along magnetic field lines. Since bremsstrahlung emission depends on the density of the ambient medium, solar HXR emission is largest when electrons are stopped by the solar "surface". Electron beams entering the chromosphere

Further author information: (Send correspondence to S. Krucker or S. Christe)
S. Krucker: E-mail: krucker@ssl.berkeley.edu, Telephone: 1 510 643 3101
S. Christe: E-mail: steven.d.christe@nasa.gov, Telephone: 1 301 286 7999

lose energy quickly through collisions, producing relatively intense HXR emission at the footpoints of magnetic field lines. Energetic electrons moving in the relatively tenuous corona suffer only a few collisions, losing little energy and producing only faint HXR emission. Present-day instruments do not have the sensitivity to see faint HXR emission from electrons traveling through the corona, nor the dynamic range to see such faint emission in the presence of bright HXR footpoint emission in the chromosphere. Existing observations therefore show us only where energetic electrons are stopped but not where they are accelerated, nor along what path they escape from the acceleration site. Thus, to make the next breakthrough in understanding the acceleration process requires HXR imaging with much higher sensitivity and dynamic range. HXR focusing optics can provide both.

Table 1. FOXSI Overview

Optics Characteristics:	
Angular Resolution (FWHM)	$\sim$7 arcsec
Number of modules	7
Number of shells per module	7 (10)
Focal length	2 m
Optics Type	Wolter I
FWHM field of view	16.6×16.6 arcmin^2
Detector Characteristics:	
Type	Double-sided Si (CdTe) Strip Detectors
Dimensions	128×128 strips or 9.6×9.6 mm^2
Detector Pitch	75 μm
Thickness	500 μm
Power	0.26 W per detector
Energy Resolution (FWHM)	$\sim$0.5 keV
Telescope Characteristics	
Energy range	$\sim$5 to 15 keV
Pixel size	7.5 arcsec
Field of View	16×16 arcsec^2
Sensitivity ($\sim$8 keV)	$\sim$0.004 (0.0032) ph cm^{-2} s^{-1} keV^{-1} or $\sim$50 times RHESSI
Dynamic Range	100 for source separation $>$ 30 arcseconds
System Effective Angular Resolution (FWHM)	$\sim$10 arcsec
Optics Effective Area	$\sim$150 cm^2 ($\sim$200) at 8 keV, $\sim$14 cm^2 ($\sim$40) at 15 keV
Overall Effective Area	$\sim$120 cm^2 ($\sim$155) at 8 keV, $\sim$8 cm^2 ($\sim$40) at 15 keV
Mission Characteristics	
Launch	January 2012 from White Sands Test Facility, NM
Observation time	$\sim$360 s

*Values in parenthesis are for FOXSI-2.

The most sensitive solar HXR observations so far are provided by the Reuven Ramaty High Spectroscopic Imager (RHESSI).[1] These measurements are obtained with a non-focusing, rotation modulation collimator (RMC) imaging technique.[2] RMCs and other types of non-focusing imaging, however, have intrinsically limited dynamic range and sensitivity. Through focusing both of these limitations can be overcome. Recent developments in x-ray focusing optics have extended the range of focusable energies well into the HXR range. New focusing x-ray optics telescopes have been developed at the Marshall Space Flight Center (MSFC) and successfully flown on balloon project called HERO to observe astrophysical objects.[3,4] Coupled with new position-sensitive solid state detectors provided by JAXA/ISAS which can do spectroscopy on individual pixels, new HXR observations with unprecedented sensitivity and dynamic range are now possible. We present a new instrument which applies these technologies to solar observations via a sounding rocket payload.

Called FOXSI, short for the Focusing Optics x-ray Solar Imager, this instrument will feature an array of grazing-incidence mirror modules focusing to a corresponding array of silicon focal plane detectors. FOXSI is expected to be $\sim$50 times more sensitive than RHESSI at 10 keV with a dynamic range of $\sim$100 for sources

separated by 30″. The high sensitivity of FOXSI will for the first time allow a search for HXR counterparts of thermal brightenings seen in the quiet corona[5–7] to evaluate the importance of heating the solar corona by nanoflares.

2. OVERVIEW

FOXSI is a sounding rocket program funded by the NASA Low Cost Access to Space (LCAS) program. Led by the Space Sciences Laboratory (SSL) at U.C. Berkeley, the FOXSI program also involves the NASA Marshall Space Flight Center (MSFC), and the Astro-H team (ISAS/JAXA).[8–11] FOXSI will apply new HXR focusing optics developed for astrophysical observations to solar observations. A major goal of the FOXSI program is to push these developing technologies to the unique requirements of solar observations; the most important of which are (1) high sensitivity, (2) good angular resolution, (3) large dynamic range, and (4) fast counting rates.

The tasks of the FOXSI program are neatly divided among the various institutions involved. The optics are being developed and manufactured at the MSFC (Section 4). The FOXSI detectors are being developed as part of the Astro-H mission[10–13] (Section 5). They consist of silicon Double-Sided Strip Detectors (DSSD) which are fabricated by Hamamatsu and read out by Application Specific Integrated Circuits (ASICs) designed and built by Gamma Medica-Ideas (Norway). SSL is leading the FOXSI program and is designing and constructing the physical payload, including the detector read-out electronics.

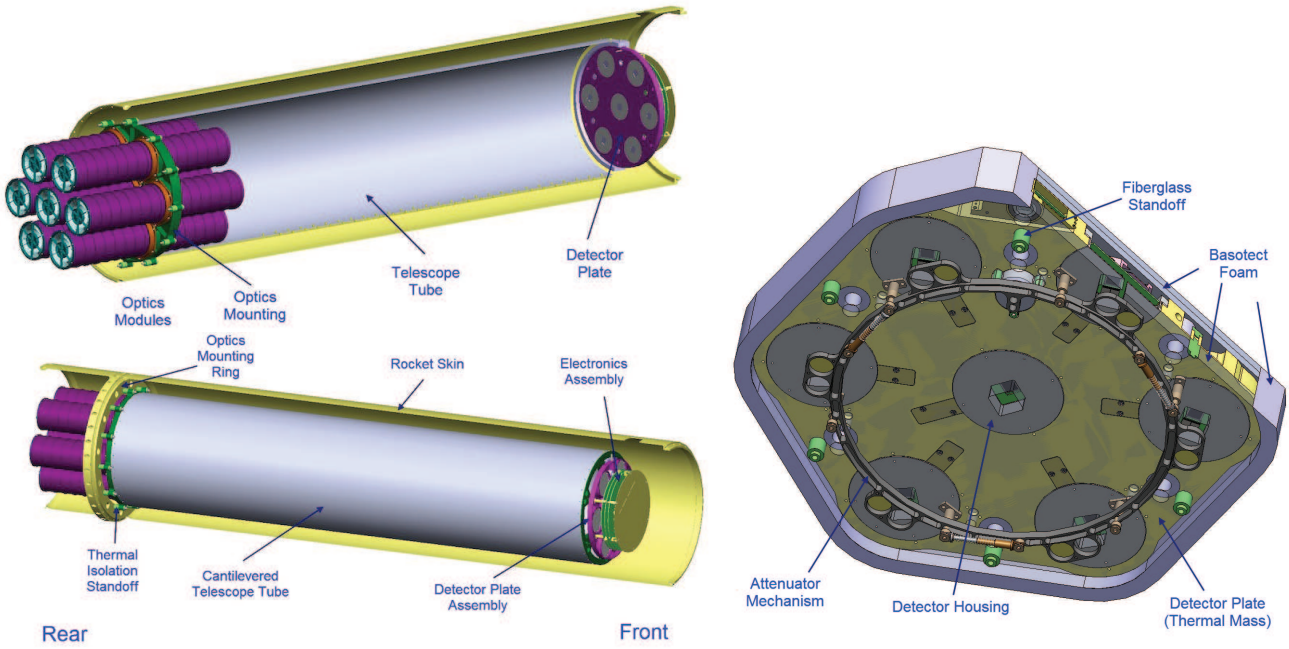

Figure 1. Diagram of the payload inside a 22 in. rocket skin. *Right Top*: The basic structure of the payload consists of a 2-m-long rolled aluminum tube (shown in cutaway) that hold the array of 7 optics and 7 detectors, mounted on an aluminum ring at one end, and an aluminum plate holding the 7 detectors at the opposite end. The payload will be oriented "backwards" within the rocket as the detector end is located at the front of the rocket. Separation of the rocket engine will allow the optics to be revealed. *Right Bottom*: The aluminum tube is made rigid at its ends by the optics mounting plate and the focal plane mounting ring (both shown in green) and this structure is cantilevered inside the rocket skin by a larger mounting ring (yellow) that is fastened to the rocket skin. The detector electronics are mounted on aluminum standoffs forward of the detectors. *Left*: Detail of the detector plane showing the detector housings as well as the attenuator mechanism.

The FOXSI instrument is composed of 7 grazing-incidence telescope modules, each with 7 nested shells. Due to constraints imposed by the rocket payload size, the FOXSI focal length is 2 m. This (relatively) short focal length limits the highest energy at which significant area can be achieved to about 20 keV, which matches well with the efficiency provided by the silicon detectors. The total effective area is expected to be ∼150 cm^2 from

$\sim$5 to 10 keV, falling to $\sim$14 cm^2 at 15 keV (Figure 2). FOXSI will have a total field of view of 960$\times$960 arcsec (HPW) which covers approximately a quarter of the solar disk. The angular resolution (FWHM) for previously flown HERO modules containing multiple nested shells is $\sim$12 arcseconds, which is limited by misalignment between the component shells. A new mounting technique developed for FOXSI improved the alignment process (see Section 4) so that the resolution of a module is now close to that of individual shells (7 arcseconds). A 128$\times$128 strip, 500 μm thick double-sided silicon strip detector with 75 μm strip pitch will cover the detector plane. The expected energy resolution of FOXSI is around 0.5 keV. The combination of low background count rates due to the small detector size and large effective area leads us to expect that the sensitivity of FOXSI will be $\sim$50 times better than RHESSI. Table 1 summarizes the properties of FOXSI. A second flight and upgrade to FOXSI has already been funded (FOXSI-2).

3. PAYLOAD DESIGN

The FOXSI payload design is heavily influenced by the existing HERO design.[3] The payload will be oriented "backwards" in the rocket casing in order to minimize rocket separation events. Shedding of the last rocket engine will reveal a hinged door that opens to the FOXSI optics. Pointing control systems will then reorient the payload sunward. The NASA-provided Solar Pointing Attitude Rocket Control System (SPARCS) system will provide high-stability programmable solar pointing. Located fore of the detector end of the payload are various rocket control systems and the rocket nose cone containing a recovery parachute. Since recovery of the payload is required the launch will take place at the NASA White Sands Test Facility in New Mexico.

The design of the FOXSI payload is driven by two basic mechanical requirements to the telescope assembly: it must properly position the seven telescope modules with their respective detectors and it must provide an optimal thermal environment for the telescope components. Structurally, the telescope modules mount to a circular aluminum plate, approximately 17 in. in diameter (see Figure 1), which in turn is riveted to a precision rolled aluminum tube that spans the entire 2 m focal length. The opposite end of the tube is riveted to a ring, to which a detector platecontaining the seven detectorsis fastened. The rigidity of the tube and the two riveted ends provides the axial alignment of the telescope modules with the detectors. This tube assembly mounts to the rocket only from the optical end, via a larger aluminum plate that is fastened directly to the rocket skin. The detector end of the tube is cantilevered so that it will not be structurally indeterminate, and also to not have any conductive thermal contact with the rocket skin.

Thermally, the optics require a stable temperature while the detectors must be kept below -20°C, and the detector electronics need a temperature between 0 and 50°C. During flight, the rocket skin will heat up to 150°C. The optics temperature is not expected to change while the detectors will be cooled passively. The detectors are mounted in the much larger thermal mass of the mounting plate. Prior to launch, the temperature of this plate will be actively cooled to -30°C with LN2, which will be piped into a sealed channel inside the plate from a dewar external to the rocket. The vaporized nitrogen will then pass into the cavity where each detector is held in order to prevent the build up of water moisture while the rocket is in its pre-launch preparations. The active and passive cooling of the optics and detector assemblies is aided by placement of insulating materials. Each telescope module is completely surrounded by a blanket of multi-layered insulation (MLI), which blocks most of the radiative heat transfer and the optics mounting plate is conductively isolated from the mounting ring by fiberglass standoffs. The detector plate is surrounded by a one-half in. layer of Basotect foam11 that is in turn covered with aluminized mylar. The detector plate is also thermally isolated from its mounting ring by a set of fiberglass standoffs. The detector electronics, which generate $\sim$10 W of heat, are mounted on aluminum standoffs that fastenand conduct heatto the focal plane mounting ring, while being insulated with foam from the detector plate. Finally, the entire telescope tube assembly is wrapped in a blanket of MLI that cuts down radiative heat transfer from the rocket skin. Thermal modeling predicts that, during the 6 min. flight, the temperature of the detector plate will rise less than 2°C from its starting temperature of -30°C. The detector assembly is also fitted with an attenuator mechanism (see Figure 1). In the case of high X-Ray flux that would saturate the detectors, an actuator will release a spring-loaded ring that will rotate a thin foil in front of each detector, significantly reducing the x-ray flux.

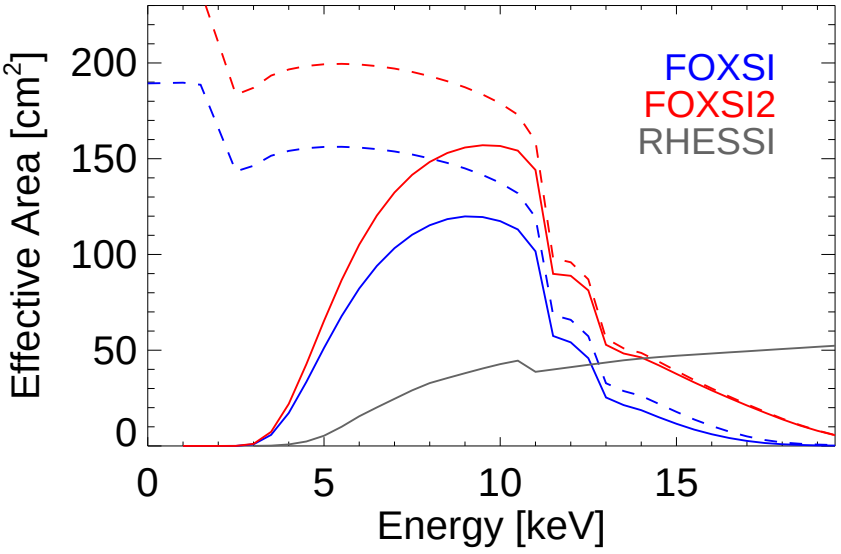

Figure 2. The expected total effective area of FOXSI as a function of energy. The dashed line represents the area provided by the optics while the solid line includes detector efficiency and absorption by thermal blanketing. The effective area for the future FOXSI-2 is also shown as well that provided by RHESSI for comparison. At 10 keV, FOXSI has 3 times the effective area of RHESSI. The future FOXSI-2 will have 4 times the effective area of RHESSI at 10 keV. In addition, the low background expected in FOXSI implies that FOXSI should be 50 times more sensitive than RHESSI.

4. OPTICS

The FOXSI grazing-incidence x-ray optics have been fabricated using an electroformed nickel replication (ENR) process.[4,14] In this process, thin nickel-alloy mirror shells are electroformed on to superpolished and figured mandrels, from which they are later separated by cooling. ENR represents a relatively-low-cost alternative to conventional figuring and polishing of individual bulky mirror shells (as was done with the sub-arcsecond resolution optics for the Chandra x-ray observatory), trading angular resolution for ease of fabrication (and hence cost). Further, the thin, light-weight shells resulting from ENR permit heavy nesting, a requirement for higher energies where small graze angles lead to low effective areas per mirror shell. A good example of this is the MSFC HERO x-ray astronomy balloon payload,[3] where 112 iridium-coated ENR-fabricated mirror shells are used to provide sensitive observations in the 20-75 keV energy band.

Table 2. Detailed Optics characteristics.

Focal length	2 m
Form	Wolter I
Number of shells	7 (10)
Outer shell radius	51.51 mm
Inner shell radius	37.99 mm (32.48 mm)
Shell length	60 cm
Shell thickness	250 μm
Coating	30 nm Iridium

*Values in parenthesis are for FOXSI-2.

The size of the FOXSI mirrors is set by the energies of interest and the available payload envelope. With 2 m focal length, a configuration of seven nested shells having diameters ranging from ∼70 to ∼100 mm was chosen, giving useful response up to ∼15 keV. Table 2 gives the parameters of a single FOXSI mirror module

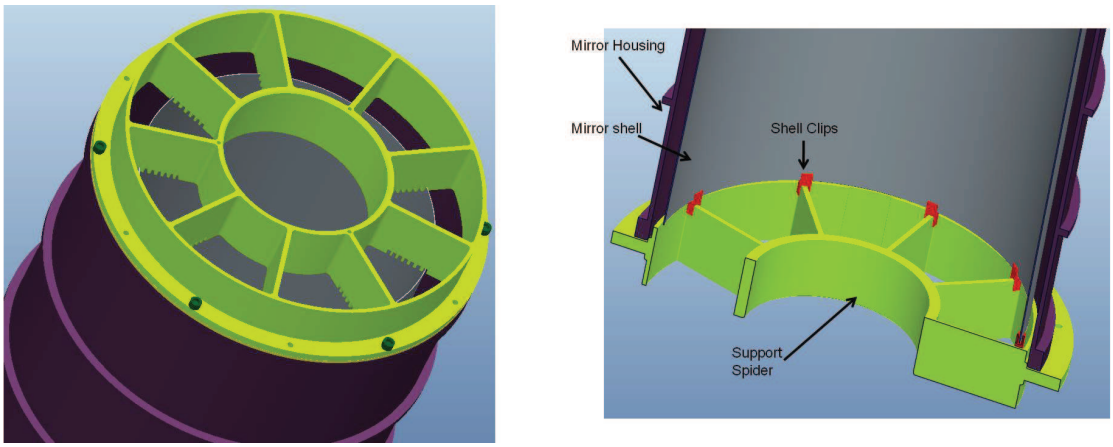

Figure 3. *Left*: Left: Graphic showing an individual shell held in grooves by the rear support spider (green). *Right*: Graphic showing an individual shell held in place by clips (red) on the front support spider.

and Figure 2 shows the total effective area of the FOXSI payload (7 modules).

For the planned FOXSI solar science goals the ability to image faint emission close to regions of intense activity is key. This effective large-contrast capability is set by the point spread function of the optics, a useful measure of which is the mirrors full width at half maximum height (FWHM) value. For FOXSI, the goal is to have a system FWHM of less than 10 arcsec which, removing the detector resolution, requires the optics to have a FWHM of 8 arcsec or less. Achieving this in individual thin mirror shells is relatively straight forward but not in telescope modules as mounting them without degrading the intrinsic resolution is a challenge. This is complicated by the fact that the mirrors are subject to severe mechanical loads during the launch of the sounding rocket (larger than those imparted during a standard launch of a satellite). Mirror-shell resonances can greatly increase the bond-joint loads during and this necessitates careful design of the mirror shell to support-spider interface.

The solution for optics mounting was to utilize special clips to attach each mirror shell to the entrance-aperture spider. These clips spread the launch loads and in addition mitigate the effects of epoxy shrinkage which can distort the mirror shell. In use, the clips are first glued to the shell in their correct locations using the spider simply as a template, from which it is later removed. Then, assembly takes place, as described below, during which the other side of the clips are permanently glued to the spider spokes. During this operation the shell clips straddle the spider spoke and so any epoxy shrinkage acts circumferentially on the shell rather than radially. This reduces potential epoxy-shrinkage-induced axial figure errors. A cartoon showing the clip arrangement on a single mirror shell is shown in Figure 3.

The mirror shell assembly is carried out on an integration stand (see Figure 4) that utilizes Keyence proximity sensors, accurate to 0.1 micron, to monitor the circularity of the shell in real time throughout the bonding process. During assembly the shells are lowered in to place and held at three points on micropositioners, which are subsequently adjusted to obtain circularity at three monitored locations (the two ends and the intersection of the shell). When circularity is obtained, a UV-cure epoxy is used to fasten the shell clips to the spider spokes, above which the shell is being suspended. After this, the micropositioners are adjusted for the next (larger) shell, and the process is repeated.

When all the 7 mirror shells are attached to the base spider, the assembly is removed from the integration stand, the housing is attached and a top spider is dropped in place. The mirror shells sit in grooves in this spider and an RTV compound is injected in the slots to provide a cushion to limit movement of the top of the shells under launch vibrations.

The alignment and assembly process for the 7 FOXSI flight mirror modules has been completed (see Figure 4) and the units have recently been vibration tested and calibrated. Early modules were tested both before and after vibration, with no detectable difference in performance. All modules were calibrated after the mechanical testing was complete.

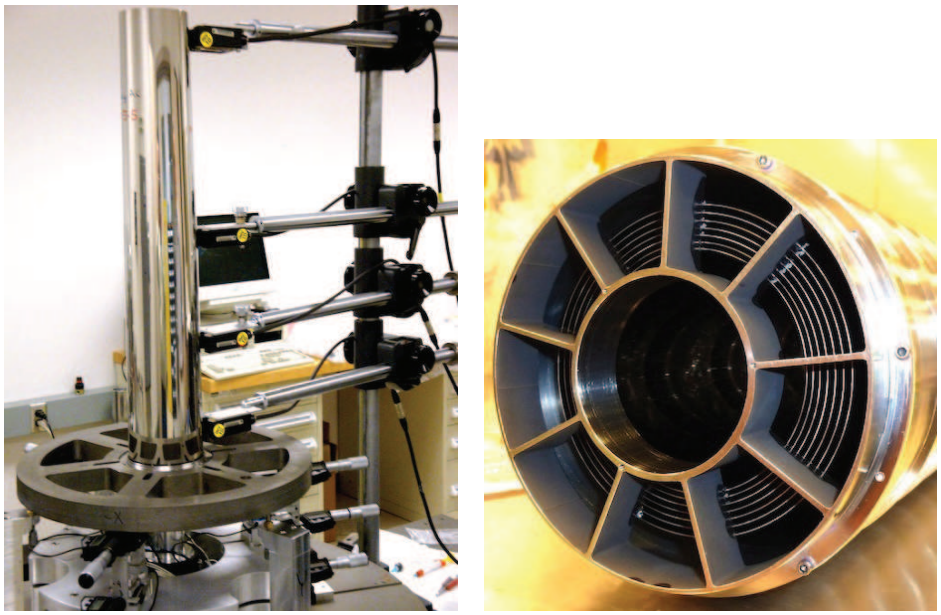

Figure 4. *Left:* Photograph of the mirror shell assembly integration stand. The stand makes use of Keyence proximity sensors, accurate to 0.1 micron, to monitor the circularity of the shell in real time throughout the bonding process. During assembly the shells are lowered in place from smallest to largest and held at three points by micropositioners which are adjusted to maintain circularity. A UV-cure epoxy is used to fasten the shell clips to the spider spokes, above which the shell is suspended. *Right:* A photograph of a completed FOXSI telescope module.

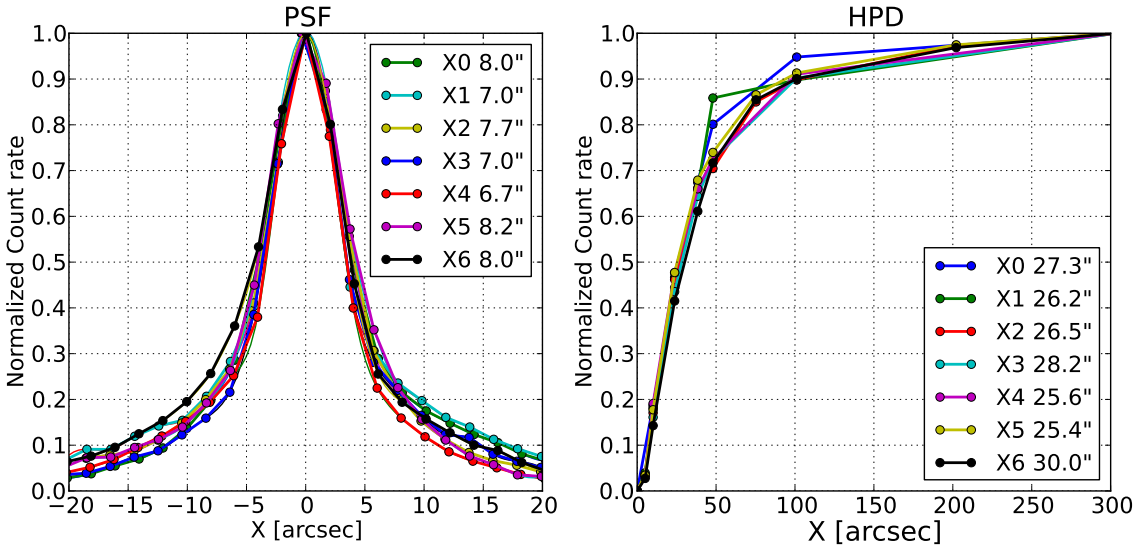

Figure 5. *Left*: The measured point spread function for all FOXSI telescopes modules. Measurements of the FWHM values are shown next to the module names (X0, X1, X2, etc.) in the legend. The FWHM values were found to be very consistent between modules and varied from ∼7 to ∼8 arcsec. Deconvolving these measurements from the test detector aperture size, implies actual FWHM of 5 to 6 arcsecond. *Right* Measurements of the half-power diameter (HPD) for each FOXSI telescope module. The HPD was found to vary from ∼25 to ∼30 arcsec.

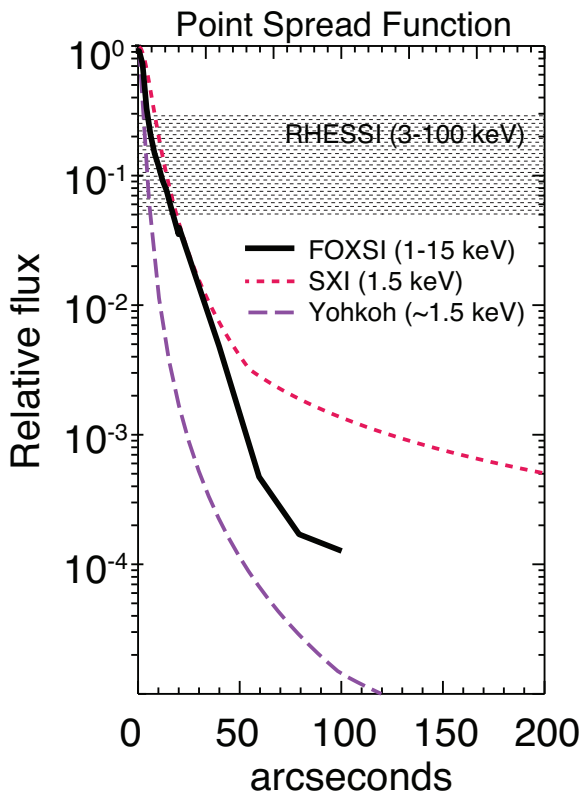

Figure 6. The measured point spread function (PSF) for a single FOXSI telescope module compared to other similar x-ray instruments. RHESSI is the only non-focusing imager and the only solar instrument in the HXR range. RHESSI's dynamic range is variable. Depending on statistics it varies from 20 in the best of cases down to 5 for statistics-limited events. The FOXSI PSF falls off rapidly; 2 orders of magnitude within ~30 arcsec and around three orders by 60 arcsec. These values imply a dynamic range of 100 to 1000 for solar flare observations.

The resulting measured resolution data for the seven flight modules are shown in Figure 5, obtained by scanning a 50 micron (~5 arcsec effective size) pinhole across the focal plane. The data show that the modules are quite consistent in performance and meet the angular resolution requirement for the FOXSI mission. Deconvolving the measured FWHM of 7 to 8 arcsec from the pinhole size gives a angular resolution of a single module between 5 and 6 arcsec. A measured full point spread function for a single module is shown and compared to other x-ray imagers in Figure 6. Solar HXR observations frequently contain multiple sources in the same field of view. The shape of the PSF is therefore very important since a single source may contribute a significant "background" for nearby sources. The PSF sets the maximum dynamic range possible. From Figure 6 it can be seen that the measured source flux falls rapidly: 2 orders of magnitude within 30 arcsec and around three orders by 60 arcsec, giving a dynamic range of 100 to 1000 for solar flare observations. This performance contrast with instruments that do not use direct imaging, such as RHESSI, which are limited to dynamic ranges of typically 5-10.

5. DETECTORS

The FOXSI program requires a focal plane detector with good energy and angular resolution, low background, and low power consumption. To meet these requirements, FOXSI uses thin double-sided silicon strip detectors (DSSDs) with a fine pitch and low-power front-end ASIC. These detectors were originally developed for the Hard x-ray Imager onboard the Astro-H (formerly NeXT) mission.[10–13]

The DSSDs are fabricated (at Hamamatsu Photonics, Japan) by implanting orthogonal n- and p-wells on either side of a monolithic silicon wafer, resulting in sets of segmented strips. An energy deposition event creates electron hole pairs which drift to opposite sides of the silicon. Due to the orthogonality of the strips, capture of the electrons and holes reveals the 2 dimensional position of the event. The FOXSI detectors have a pitch of 75 μm, corresponding to a angular resolution of ~8 arcseconds at a focal length of 2 m, matching the optical resolution of a telescope module (7 arcseconds). With a total of 128 strips on each side, the total active area

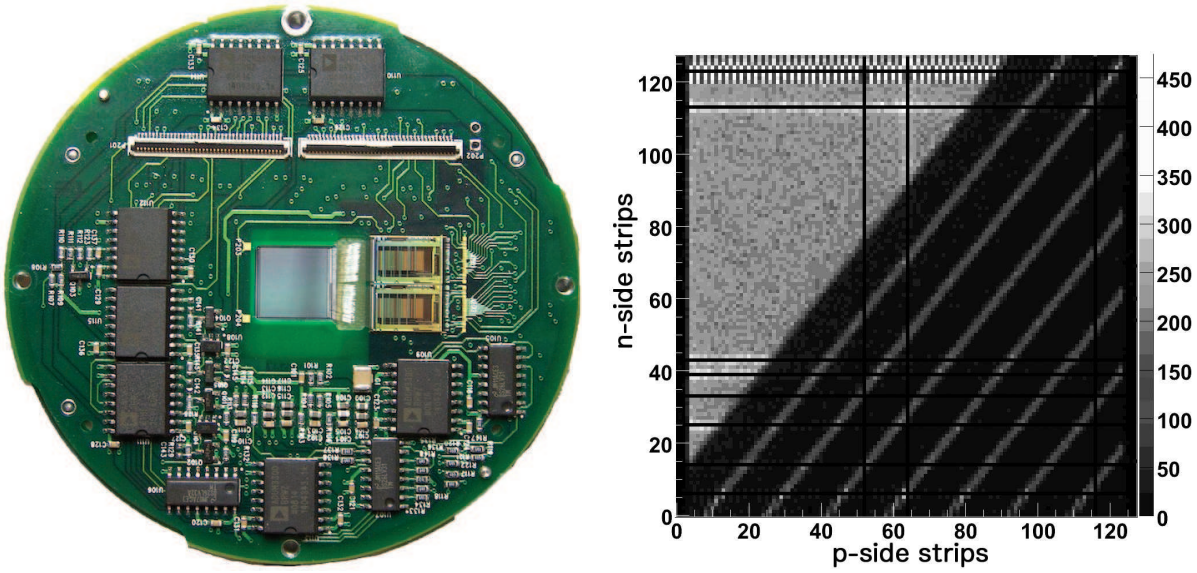

Figure 7. *Left:* A FOXSI flight detector board with ASICs and detectors wirebonded. The ASICs can be seen to the right of the detector. *Right:* Shadow image on a prototype FOXSI detector using a ^{133}Ba source and a tungsten plate with 0.1 mm-wide slits.[15] Some dark lines are due to missed wirebonds; the checkered pattern at the top shows pad locations.

is 9.6×9.6 mm^2 while the total sensor size is 11.7×11.7 mm^2. The detector thickness is 500 μm, providing an efficiency of 98% at 10 keV and 68% at 15 keV.

The DSSDs are read out using front-end ASICs (VATA451) developed as a joint effort by ISAS/JAXA and Gamma Medica-Ideas. For each DSSD, four ASICs read out a total of 256 strips (128 strips on each side). When an energy deposition event occurs, a fast shaper (0.6 μs shaping time) and discriminator produce an analog trigger. A slow shaper (3 μs shaping time) with sample-and-hold circuitry then measures the deposited energy. In this way, data are collected on a per-photon basis. After each trigger, the entire detector is read out.

The ASICs perform A to D conversion using Wilkinson-style ramp ADCs and produce a binary map showing which strips have triggered, along with 10-bit data for each channel, a common-mode noise channel, and a diagnostic channel. Since the ASIC was designed to minimize power consumption, each channel requires 1 mW per channel, for a total of 0.26 W per detector. All channels are converted simultaneously and a serial data stream is clocked out of the ASIC. The entire acquisition takes place in 185 μs. A dedicated FPGA (Actel ProASIC3) clocks the four ASICs, performs data reduction, and sends the data to a formatter (developed at SSL) for packaging into the final telemetry stream. To meet telemetry constraints (2 Mbps, or 500 photons s^{-1} det^{-1}), the FPGAs perform zero suppression and pedestal subtraction. Since charge may occasionally be shared between neighboring strips, data are retained from the strip registering the highest energy and also the adjacent strips.

Spectral and imaging tests were performed on a prototype system including a FOXSI detector and 4 ASICs at ISAS/JAXA.[15] The tests used a ^{241}Am radioactive source, an operating temperature of -20 degrees Celsius, and a bias voltage of 300 V. The energy resolution obtained were 430 eV and 1.6 keV for the p-side and n-side, respectively at 14 keV (See Figure 8.) Since the p-side channels have better energy resolution than those on the n-side (see[15] for discussion), only the p-side is used for spectral information, while both p- and n-sides are used for position information. These tests will be repeated at SSL with the FOXSI flight system prior to payload integration.

A problem unique to strip detectors is "ghosting". If photons of similar energies are simultaneously detected at two locations in the detector, four channels will trigger. From these four channels, four possible locations can be reconstructed but only two locations are valid. To mitigate this effect, each FOXSI detector is set at a different clocking angle. In this way, the ghost sources will always appear in different locations in different detectors while the true source location will be constant.

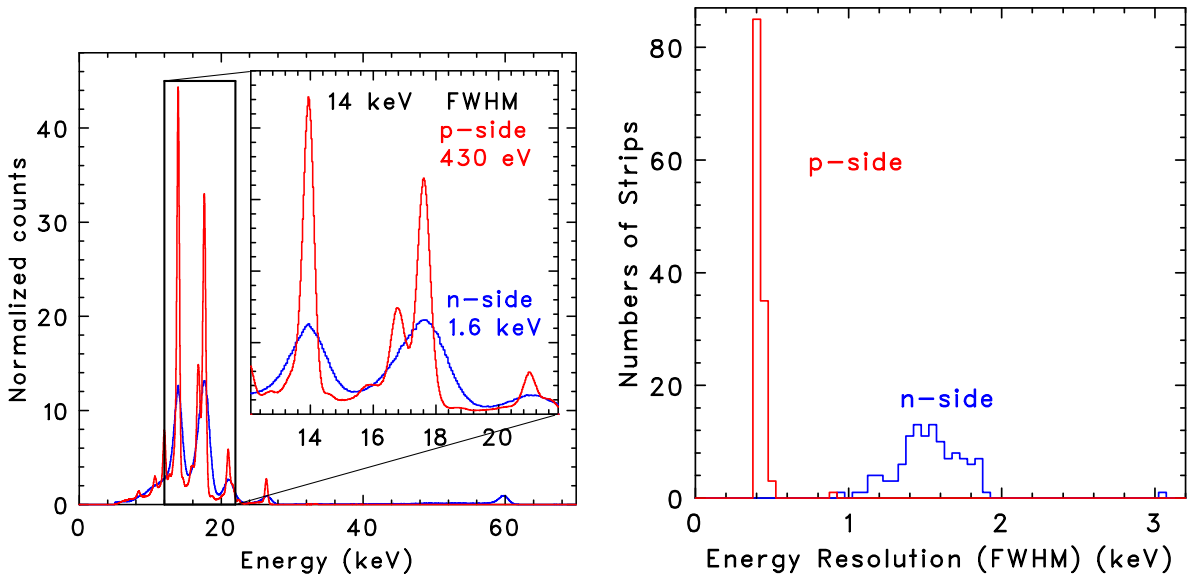

Figure 8. *Left:* Spectra from a ^{241}Am source, using a bias voltage of 300 V and an operating temperature of -20 degrees Celsius. *Right:* Histogram of energy resolutions for all the p-side and n-side channels. The higher-performing p-side will be used for energy spectra, while both the p- and n-sides will be used for positional information.[15]

6. OBSERVATIONS/SCIENCE

The main science goal of FOXSI is to explore HXR emissions from the non-flaring Sun* (for other science targets see Figure 10). The huge increase in sensitivity (a factor of 50) as compared to previous HXR imaging observations provides, for the first time, the opportunity to search in the non-flaring corona for HXR emission produced by supra-thermal (>10 keV) electrons and hot thermal plasmas (with temperatures above 8 MK). These emissions are expected to be present in the coronal heating scenario in which a large number of small flares provides the energy input to heat the solar corona. The detection of HXR emission from the non-flaring Sun would provide strong evidence for nanoflare heating, while the absence would call into question nanoflares as a solution to the coronal heating problem.

HXR emission from the non-flaring Sun is expected to be easiest to detect in the ∼5 to 15 keV range.[16] The FOXSI payload was therefore designed to have maximal effective area around 10 keV without consideration of the high energy response (see Figure 2). Restricting the energy range of FOXSI to energies below 15 keV further simplifies the instrument design as no multi-layer coatings of the grazing incidence optics are needed and Si detectors cover the energy range adequately.

Observations at around 10 keV require a minimum altitude of ∼120 km to avoid strong atmospheric absorption, giving a total observation time of ∼360 s. Thermal events seen in EUV in the quiet Sun indicate heating on time scales of minutes.[6] From EUV observations,[17–19] we estimate ∼10 to ∼1000 such events within the FOXSI field of view ($960'' \times 960''$) during the flight. The angular resolution of FOXSI will allow us to separate individual events without resolving them. If these quiet-Sun events are similar to regular active-region solar flares, FOXSI should clearly detect non-thermal bremsstrahlung emission from the supra-thermal electrons (Figure 9). The absence of HXR emission would indicate that the thermal EUV events in the quiet Sun are different from regular flare seen in active regions.

As the FOXSI field-of-view is smaller than the solar disk by a factor of 4, target selection is important. To ensure that the HXR optics are working properly, the first target (for ∼60 seconds) will be an active region that is hot enough to produce a clear signal. The second target for the remaining time (∼300 seconds) will include quiet Sun and polar areas, avoiding active regions. In the unlikely case that the count rates for the second target

*The difficulty of predicting solar flares together with a restrictive launch window and the short observation time provided by sounding rockets excludes solar flares as a main science goal.

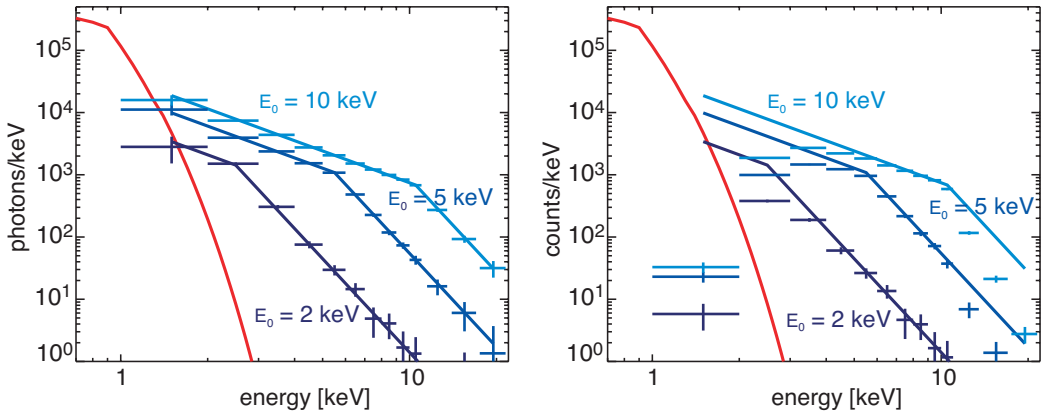

Figure 9. *Left*: Expected x-ray photon spectrum of a quiet Sun nanoflare assuming the heating observed in SXR (T=2 MK, EM=10^{44} cm^{-3}, $E_{thermal} = 5\times10^{25}$ergs, duration of 60 s) is produced by non-thermal electrons. Three spectra for different turn-over energies are shown. The photon spectrum is assumed to be a power law with a slope of -5 above the turnover energy, E_0, and a slope of -1.7 below. The blue lines show the non-thermal spectra with perfect statistics and resolution; the blue data points with error bars are the expected FOXSI measurements. The red curve shows the thermal spectra (T=2 MK). *Right*: The count spectrum. At low energies, photons are absorbed by a beryllium entrance window while at high energies the effective area of the telescope is reduced. The expected count rate for the three spectra shown are 14, 91, 245 counts per second, respectively.

are too high for the FOXSI data rate (i.e. above 300 counts s^{-1} det^{-1}), mechanical attenuators can be put in front of the detectors to reduce the low energy photon flux.

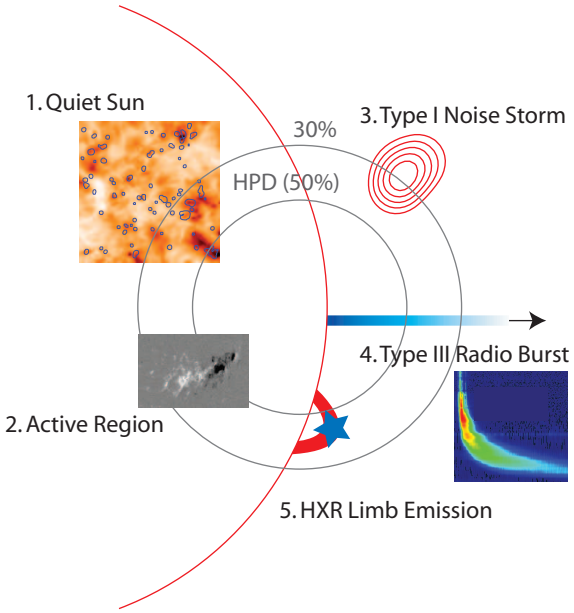

Figure 10. An illustration of possible FOXSI science targets compared to the field-of-view. The field of view is defined as the half power diameter (grey circles). The 30% level contour is also plotted. The main goal for FOXSI is to observe non-thermal electrons through their HXR emission. The primary science targets are the (1) quiet Sun and (2) active-region microflares. Other targets associated with non-thermal electron emission, in order of importance, are type I noise storms (3), type III radio bursts (4), and flare loop-top emission (5).

7. OUTLOOK AND CONCLUSIONS

HXR grazing-incidence focusing optics are expected to provide the sensitivity and dynamic range needed to image typical solar electron beams as they travel through the corona and image their acceleration region. FOXSI is slated for launch in January 2012 and is expected to be a pathfinder for a future space-based satellite mission. Such a mission will be able to image where electrons are accelerated, along which field lines they travel away from the acceleration site, where they are stopped, and how some electrons escape into interplanetary space. Additionally, spectroscopy will simultaneously provide quantitative measurements such as the energy spectrum, density, and energy content of the accelerated electrons. Such observations will revolutionize our understanding of particle acceleration in astrophysical plamsas.

The FOXSI payload will be recovered and a second scientific flight in 2013 is already funded (FOXSI-2). For the second flight, the effective area will be increased by the addition of three more inner shells to each telescope module (see Figure 2). In addition, the silicon detectors will be replaced by Cadmium Telluride (CdTe) strip detectors[20] again provided by the Astro H team. For longer duration observations that will allow us to observe solar flares, balloon and satellite versions of FOXSI are currently under study. FOXSI is part of two missions under study in the decadal review (SEE2020 and RAM) as well as a concept study developed for the European Space Agency (SPARXS). For such missions, the use of high Z detectors such as CZT or CdTe (strips or pixels) is essential. Such a system may also make astrophysical observations, and a combined mission in astrophysics and heliophysics is a possibility that should be considered.

ACKNOWLEDGMENTS

This effort is funded by NASA grant NNH06ZDA001N. R. P. Lin was also supported in part by the WCU grant (No. R31-10016) funded by the Korean Ministry of Education, Science, and Technology.

REFERENCES

1. Lin, R. P., Dennis, B. R., Hurford, G. J., Smith, D. M., Zehnder, A., Harvey, P. R., Curtis, D. W., Pankow, D., Turin, P., Bester, M., Csillaghy, A., Lewis, M., Madden, N., van Beek, H. F., Appleby, M., Raudorf, T., McTiernan, J., Ramaty, R., Schmahl, E., Schwartz, R., Krucker, S., Abiad, R., Quinn, T., Berg, P., Hashii, M., Sterling, R., Jackson, R., Pratt, R., Campbell, R. D., Malone, D., Landis, D., Barrington-Leigh, C. P., Slassi-Sennou, S., Cork, C., Clark, D., Amato, D., Orwig, L., Boyle, R., Banks, I. S., Shirey, K., Tolbert, A. K., Zarro, D., Snow, F., Thomsen, K., Henneck, R., McHedlishvili, A., Ming, P., Fivian, M., Jordan, J., Wanner, R., Crubb, J., Preble, J., Matranga, M., Benz, A., Hudson, H., Canfield, R. C., Holman, G. D., Crannell, C., Kosugi, T., Emslie, A. G., Vilmer, N., Brown, J. C., Johns-Krull, C., Aschwanden, M., Metcalf, T., and Conway, A., "The Reuven Ramaty High-Energy Solar Spectroscopic Imager (RHESSI)," Sol. Phys. **210**, 3–32 (Nov. 2002).
2. Hurford, G. J., Schmahl, E. J., Schwartz, R. A., Conway, A. J., Aschwanden, M. J., Csillaghy, A., Dennis, B. R., Johns-Krull, C., Krucker, S., Lin, R. P., McTiernan, J., Metcalf, T. R., Sato, J., and Smith, D. M., "The RHESSI Imaging Concept," Sol. Phys. **210**, 61–86 (Nov. 2002).
3. Ramsey, B. D., Alexander, C. D., Apple, J. A., Benson, C. M., Dietz, K. L., Elsner, R. F., Engelhaupt, D. E., Ghosh, K. K., Kolodziejczak, J. J., O'Dell, S. L., Speegle, C. O., Swartz, D. A., and Weisskopf, M. C., "First Images from HERO, a Hard X-Ray Focusing Telescope," ApJ **568**, 432–435 (Mar. 2002).
4. Ramsey, B. D., "Replicated Nickel Optics for the Hard-X-Ray Region," *Experimental Astronomy* **20**, 85–92 (Dec. 2005).
5. Krucker, S. and Benz, A. O., "Are Heating Events in the Quiet Solar Corona Small Flares? Multiwavelength Observations of Individual Events," Sol. Phys. **191**, 341–358 (Feb. 2000).
6. Krucker, S., Benz, A. O., Bastian, T. S., and Acton, L. W., "X-Ray Network Flares of the Quiet Sun," ApJ **488**, 499–+ (Oct. 1997).
7. Berghmans, D., Clette, F., and Moses, D., "Quiet Sun EUV transient brightenings and turbulence. A panoramic view by EIT on board SOHO," A&A **336**, 1039–1055 (Aug. 1998).

8. Kokubun, M., Nakazawa, K., Enoto, T., Fukazawa, Y., Gilmore, K., Kataoka, J., Kawaharada, M., Laurent, P., Lebrun, F., Limousin, O., Makishima, K., Mizuno, T., Mori, K., Nakamori, T., Ohno, M., Ohta, M., Sato, G., Tajima, H., Takahashi, H., Takahashi, T., Tanaka, T., Terada, Y., Uchiyama, H., Uchiyama, Y., Watanabe, S., Yatsu, Y., and Yamaoka, K., "Hard x-ray imager (HXI) for the ASTRO-H Mission," in [*Society of Photo-Optical Instrumentation Engineers (SPIE) Conference Series*], *Society of Photo-Optical Instrumentation Engineers (SPIE) Conference Series* **7732** (July 2010).
9. Takahashi, T., Mitsuda, K., Kelley, R., Aharonian, F., Akimoto, F., Allen, S., Anabuki, N., Angelini, L., Arnaud, K., Awaki, H., Bamba, A., Bando, N., Bautz, M., Blandford, R., Boyce, K., Brown, G., Chernyakova, M., Coppi, P., Costantini, E., Cottam, J., Crow, J., de Plaa, J., de Vries, C., den Herder, J.-W., Dipirro, M., Done, C., Dotani, T., Ebisawa, K., Enoto, T., Ezoe, Y., Fabian, A., Fujimoto, R., Fukazawa, Y., Funk, S., Furuzawa, A., Galeazzi, M., Gandhi, P., Gendreau, K., Gilmore, K., Haba, Y., Hamaguchi, K., Hatsukade, I., Hayashida, K., Hiraga, J., Hirose, K., Hornschemeier, A., Hughes, J., Hwang, U., Iizuka, R., Ishibashi, K., Ishida, M., Ishimura, K., Ishisaki, Y., Isobe, N., Ito, M., Iwata, N., Kaastra, J., Kallman, T., Kamae, T., Katagiri, H., Kataoka, J., Katsuda, S., Kawaharada, M., Kawai, N., Kawasaki, S., Khangaluyan, D., Kilbourne, C., Kinugasa, K., Kitamoto, S., Kitayama, T., Kohmura, T., Kokubun, M., Kosaka, T., Kotani, T., Koyama, K., Kubota, A., Kunieda, H., Laurent, P., Lebrun, F., Limousin, O., Loewenstein, M., Long, K., Madejski, G., Maeda, Y., Makishima, K., Markevitch, M., Matsumoto, H., Matsushita, K., McCammon, D., Miller, J., Mineshige, S., Minesugi, K., Miyazawa, T., Mizuno, T., Mori, K., Mori, H., Mukai, K., Murakami, H., Murakami, T., Mushotzky, R., Nakagawa, Y., Nakagawa, T., Nakajima, H., Nakamori, T., Nakazawa, K., Namba, Y., Nomachi, M., O'Dell, S., Ogawa, H., Ogawa, M., Ogi, K., Ohashi, T., Ohno, M., Ohta, M., Okajima, T., Ota, N., Ozaki, M., Paerels, F., Paltani, S., Parmar, A., Petre, R., Pohl, M., Porter, S., Ramsey, B., Reynolds, C., Sakai, S.-I., Sambruna, R., Sato, G., Sato, Y., Serlemitsos, P., Shida, M., Shimada, T., Shinozaki, K., Shirron, P., Smith, R., Sneiderman, G., Soong, Y., Stawarz, L., Sugita, H., Szymkowiak, A., Tajima, H., Takahashi, H., Takei, Y., Tamagawa, T., Tamura, T., Tamura, K., Tanaka, T., Tanaka, Y., Tanaka, Y., Tashiro, M., Tawara, Y., Terada, Y., Terashima, Y., Tombesi, F., Tomida, H., Tozuka, M., Tsuboi, Y., Tsujimoto, M., Tsunemi, H., Tsuru, T., Uchida, H., Uchiyama, Y., Uchiyama, H., Ueda, Y., Uno, S., Urry, M., Watanabe, S., White, N., Yamada, T., Yamaguchi, H., Yamaoka, K., Yamasaki, N., Yamauchi, M., Yamauchi, S., Yatsu, Y., Yonetoku, D., and Yoshida, A., "The ASTRO-H Mission," in [*Society of Photo-Optical Instrumentation Engineers (SPIE) Conference Series*], *Society of Photo-Optical Instrumentation Engineers (SPIE) Conference Series* **7732** (July 2010).
10. Takeda, S., Takahashi, T., Watanabe, S., Tajima, H., Tanaka, T., Nakazawa, K., and Fukazawa, Y., "Double-sided silicon strip detector for x-ray imaging," *SPIE Newsroom* **DOI: 10.1117/2.1200802.0889**, (Feb. 2008).
11. Watanabe, S., Ishikawa, S.-N., Aono, H., Takeda, S., Odaka, H., Kokubun, M., Takahashi, T., Nakazawa, K., Tajima, H., Onishi, M., and Kuroda, Y., "High Energy Resolution Hard X-Ray and Gamma-Ray Imagers Using CdTe Diode Devices," *IEEE Transactions on Nuclear Science* **56**, 777–782 (June 2009).
12. Kokubun, M., Nakazawa, K., Watanabe, S., Fukazawa, Y., Kataoka, J., Katagiri, H., Mizuno, T., Makishima, K., Ohno, M., Sato, G., Sato, R., Tajima, H., Takahashi, T., Tamagawa, T., Tanaka, T., Tashiro, M., Takahashi, H., Terada, Y., Uchiyama, Y., Urata, Y., Yamaoka, K., Takeda, S., Kishishita, T., Ushio, M., Katsuta, J., Ishikawa, S., Odaka, H., Aono, H., Sugimoto, S., Koseki, Y., Kitaguchi, T., Enoto, T., Yamada, S., Yuasa, T., Ueda, T., Uehara, Y., Okuyama, S., Yasuda, H., Nishino, S., Umeki, Y., Hayashi, K., Matsuoka, M., Ikejiri, Y., Endo, A., Yaji, Y., Kodaka, N., Iwakiri, W., Kouzu, T., Sugasawara, T., Harayama, A., and Nakahira, S., "Hard X-ray imager (HXI) for the NeXT mission," in [*Society of Photo-Optical Instrumentation Engineers (SPIE) Conference Series*], *Society of Photo-Optical Instrumentation Engineers (SPIE) Conference Series* **7011** (Aug. 2008).
13. Takahashi, T., Kelley, R., Mitsuda, K., Kunieda, H., Petre, R., White, N., Dotani, T., Fujimoto, R., Fukazawa, Y., Hayashida, K., Ishida, M., Ishisaki, Y., Kokubun, M., Makishima, K., Koyama, K., Madejski, G. M., Mori, K., Mushotzky, R., Nakazawa, K., Ogasaka, Y., Ohashi, T., Ozaki, M., Tajima, H., Tashiro, M., Terada, Y., Tsunemi, H., Tsuru, T. G., Ueda, Y., Yamasaki, N., and Watanabe, S., "The NeXT Mission," in [*Society of Photo-Optical Instrumentation Engineers (SPIE) Conference Series*], *Society of Photo-Optical Instrumentation Engineers (SPIE) Conference Series* **7011** (Aug. 2008).

14. Ramsey, B. D., Elsner, R. F., Engelhaupt, D. E., O'Dell, S. L., Speegle, C. O., and Weisskopf, M. C., "Development of hard x-ray optics at MSFC," in [*Society of Photo-Optical Instrumentation Engineers (SPIE) Conference Series*], J. E. Truemper & H. D. Tananbaum, ed., *Society of Photo-Optical Instrumentation Engineers (SPIE) Conference Series* **4851**, 631–638 (Mar. 2003).
15. Ishikawa, S., Saito, S., Tajima, H., Tanaka, T., Watanabe, S., Odaka, H., Fukuyama, T., Kokubun, M., Takahashi, T., Terada, Y., Krucker, S., Christe, S., McBride, S., and Glesener, L., "Fine-pitch semiconductor detector for the foxsi mission," *Nuclear Science, IEEE Transactions on* **PP**(99), 1 –11 (2011).
16. Hannah, I. G., Hurford, G. J., Hudson, H. S., Lin, R. P., and van Bibber, K., "First Limits on the 3-200 keV X-Ray Spectrum of the Quiet Sun Using RHESSI," ApJ **659**, L77–L80 (Apr. 2007).
17. Krucker, S. and Benz, A. O., "Energy Distribution of Heating Processes in the Quiet Solar Corona," ApJ **501**, L213+ (July 1998).
18. Aschwanden, M. J., Nightingale, R. W., Tarbell, T. D., and Wolfson, C. J., "Time Variability of the "Quiet" Sun Observed with TRACE. I. Instrumental Effects, Event Detection, and Discrimination of Extreme-Ultraviolet Microflares," ApJ **535**, 1027–1046 (June 2000).
19. Parnell, C. E. and Jupp, P. E., "Statistical Analysis of the Energy Distribution of Nanoflares in the Quiet Sun," ApJ **529**, 554–569 (Jan. 2000).
20. Ishikawa, S.-n., Watanabe, S., Fukuyama, T., Sato, G., Kokubun, M., Odaka, H., Saito, S., Takahashi, T., Nakazawa, K., and Tanaka, T., "Development of Double-Sided CdTe Strip Detectors for γ-Ray Imaging and Spectroscopy," *Japanese Journal of Applied Physics* **49**, 116702–+ (Nov. 2010).